Skyrme-Hartree-Fock calculation on He, Li, and Be isotopes

Yao-song Shen and Zhongzhou Ren
Department of Physics, Nanjing University, Nanjing 210008, Peoples Republic of China
(Received 15 February 1996)

The ground-state properties of He, Li, and Be nuclei are investigated by the Skyrme-Hartree-Fock approach with new force parameters SKI4 of Reinhard and Flocard [Nucl. Phys. A **584**, 467 (1995)] plus a density-dependent pairing correlation. Calculations show that the Skyrme-Hartree-Fock model with above force parameters provides a good description on the binding energy and radii of He, Li, and Be isotopes. It also succeeds in reproducing neutron halos in nuclei ^{6}He, ^{8}He, ^{11}Li, and ^{14}Be. A detailed discussion on numerical results is provided and an explanation for the above success is given. [S0556-2813(96)02509-5]

PACS number(s): 21.10.Dr, 21.30.Fe, 21.60.Jz, 27.20.+n

I. INTRODUCTION

Recent experiments [1–3] with radioactive beams have opened a new field in nuclear physics, the study of nuclei far from the β-stable line, which are referred to as exotic nuclei. One can investigate the nuclei close to the drip lines thanks to a large variety of techniques involving new accelerators and very good isotope separators. By studies on exotic nuclei, we can test present nuclear models, such as mean-field models, and develop nuclear many-body theories.

The Skyrme-Hartree-Fock (SHF) model has enjoyed enormous success in providing an appropriate description of the ground-state properties of nuclei near the valley of stability [4–10]. In all these calculations the spin-orbit potential has been assumed to be isospin independent. However, it was pointed out in recent research [10,11] that the SHF model with standard parameters cannot reproduce the isotope shifts in the Ca, Sr, and Pb isotopes. Very recently Reinhard *et al.* [12] have analyzed the problem in detail and found they can succeed in reproducing isotope shifts for Ca, Pb, and Sr using the new force parameters SKI4 in which a simple modification of the spin-orbit interaction has been made in the SHF model.

In the standard SHF model, pairing correlations have always been treated with a constant-force approach or a constant-gap approach in BCS equations. This treatment fails to reproduce the odd-even staggering of the binding energy and the large kink of charge radii for ^{208}Pb [11], since the pairing force is especially important in open-shell nuclei. Tajima *et al.* introduced a density-dependent zero-range pairing force instead of the normal constant-force or constant-gap approach in pairing correlations and succeeded in explaining some properties of nuclei [11].

In this paper, we investigate the ground state properties of He, Li, and Be isotopes using the SHF model with the new SKI4 Skyrme-type force parameters [12] plus a density-dependent pairing correlation. For simplicity, we use the abbreviation SHFDD, corresponding to the SHF model with the set SKI4 plus a density-dependent pairing correlation. Our purposes are (i) to see whether the SHFDD description works well for light neutron-rich nuclei, (ii) to discuss the properties of some nuclei near the neutron drip line, and (iii) to study the difference between the SHFDD model and the normal SHF model. This paper is organized in the following way. Section II is a short description on the framework of the SHFDD model. In Sec. III, we have given the numerical results and the discussions. Section IV is the summary.

II. THE FRAMEWORK OF THE SKYRME-HARTREE-FOCK MODEL PLUS A DENSITY-DEPENDENT PAIRING CORRELATION

As the Skyrme-Hartree-Fock model is a standard method and all the formulations can be found in Ref. [6], here we only give a short description on the framework of the SHF model with new force parameters SKI4 [12] plus a density-dependent pairing correlation [11].

For the normal Skyrme force, the neutron density dependence is linear for the mass and spin-orbit potentials [12]

$$B_{\mathrm{SHF}}=\frac{\hbar^2}{2m}+b_1\rho+b_1'\rho_n, \tag{1}$$

$$W_{\mathrm{SHF}}=b_4(\nabla\rho+\nabla\rho_n). \tag{2}$$

Reinhard *et al.* [12] introduced an additional coefficient b_4' in the spin-orbit term in a generalized Skyrme functional:

$$\varepsilon_{ls}=-\int d^3r\left\{b_4\rho\nabla J+\sum_{q\in\{p,n\}}b_4'\rho_q\nabla J_q\right\}, \tag{3}$$

where J is a spin density and its definition can be found in Ref. [12]. The spin-orbit potential W for neutrons becomes [12]

$$W_q(r)=b_4\nabla\rho+b_4'\nabla\rho_q. \tag{4}$$

In the following calculations, we use the parameter set SKI4 because it can not only describe the ground-state properties of spherical nuclei but also reproduce isotope shifts in Ca, Sr, and Pb isotopes. The values of the parameter set SKI4 are [12] $t_0=-1855.83$, $t_1=473.829$, $t_2=1006.86$, $t_3=9703.61$, $x_0=0.4051$, $x_1=-2.8891$, $x_2=-1.3252$, $x_3=1.1452$, $b_4=183.097$, $b_4'=-180.351$, $\alpha=0.25$.

TABLE I. Binding energy, pairing energy, and various radii of He isotopes. Experimental binding energies are taken from Ref. [16]. B and PE denote the binding energy and the pairing energy, respectively.

	Expt	SHFDD				
	B (MeV)	B (MeV)	PE (MeV)	R_n (fm)	R_m (fm)	R_p (fm)
^{4}He	28.29	27.42	0.00	2.07	2.07	2.07
^{5}He	27.41	27.02	0.00	2.84	2.55	2.04
^{6}He	29.27	28.44	1.66	3.11	2.80	2.02
^{7}He	28.82	27.94	0.00	3.21	2.92	2.01
^{8}He	31.41	29.30	0.07	3.25	2.98	2.01
^{9}He	30.26	28.46	0.00	3.55	3.27	2.04
^{10}He		28.21	0.00	3.63	3.38	2.08

Now, we give a description for a density-dependent pairing correlation, which is especially important in open-shell nuclei. We use a density-dependent zero-range pairing force [11]:

$$V^\tau(\mathbf{r}_1,\sigma_1,\mathbf{r}_2,\sigma_2)=V_0^\tau\frac{1-\sigma_1\cdot\sigma_2}{4}\delta(\mathbf{r}_1-\mathbf{r}_2)f\left(\frac{\mathbf{r}_1+\mathbf{r}_2}{2}\right), \quad (5)$$

where the superscript $\tau=p(n)$ denotes protons (neutrons) and $f(\mathbf{r})$ is a density-dependent function which has a linear form [11], $f(\mathbf{r})=1-\rho(\mathbf{r})/\rho_0$. ρ_0 is a reference density.

The pairing matrix element of neutrons and protons is written as

$$\begin{aligned}V^\tau_{i\bar{i}j\bar{j}}&=\int d\mathbf{r}_1 d\mathbf{r}_2\sum_{\sigma_1,\sigma_2}\phi_i^*(\mathbf{r}_1,\sigma_1)\phi_{\bar{i}}^*(\mathbf{r}_2,\sigma_2)V^\tau\\&\quad\times[\phi_j(\mathbf{r}_1,\sigma_1)\phi_{\bar{j}}(\mathbf{r}_2,\sigma_2)-\phi_{\bar{j}}(\mathbf{r}_1,\sigma_1)\phi_j(\mathbf{r}_2,\sigma_2)]\\&=V_0^\tau\int\sum_{\sigma_1}|\phi_i(\mathbf{r}_1,\sigma_1)|^2\sum_{\sigma_2}|\phi_j(\mathbf{r}_2,\sigma_2)|^2 f(\mathbf{r})d\mathbf{r}\\&=V_0^\tau\int d\mathbf{r}\rho_i(\mathbf{r})\rho_j(\mathbf{r})f(\mathbf{r}), \quad (6)\end{aligned}$$

where $\rho_i(\mathbf{r})=|\phi_i(\mathbf{r})|^2$ and $\phi_i(\mathbf{r})$ is the wave function of the ith single-particle orbit.

As in [13,14], it is necessary to prevent the unrealistic pairing of highly excited states, and to confine the region of the influence of the pairing potential to the vicinity of the Fermi surface. It is accomplished by defining the contribution E_p to the total energy as

$$E_p^\tau=\sum_{ij} f_i u_i v_i V^\tau_{i\bar{i}j\bar{j}} f_j u_j v_j,$$

$$f_i=\left[1+\exp\left(\frac{\varepsilon_i-\lambda-\Delta\varepsilon}{\mu}\right)\right]^{-1}, \quad (7)$$

where u_i and v_i are occupying factors [11,13]. f_i is a cutoff factor with $\Delta\varepsilon=5$ MeV and $\mu=0.5$ MeV [13]. The numerical results are fairly insensitive to the above two values of $\Delta\varepsilon$ and μ [13]. With this definition of the pairing energy, the state-dependent energy gaps Δ_i^τ are solutions of following equations [13]:

$$\Delta_i^\tau=-\frac{1}{2}\sum V^\tau_{i\bar{i}j\bar{j}}\frac{f_j^2\Delta_j^\tau}{\sqrt{(\varepsilon_i-\lambda)^2+f_j^2\Delta_j^{\tau^2}}}. \quad (8)$$

The pairing energy and occupation probabilities are written as [13]

$$E_p^\tau=-\frac{1}{2}\sum\frac{f_j^2\Delta_j^{\tau^2}}{\sqrt{(\varepsilon_i-\lambda)^2+f_j^2\Delta_j^{\tau^2}}},$$

$$v_i^2=\frac{1}{2}\left[1-\frac{\varepsilon_i-\lambda}{\sqrt{(\varepsilon_i-\lambda)^2+f_j^2\Delta_j^{\tau^2}}}\right]. \quad (9)$$

In calculations, we first calculate the matrix elements in Eq. (6), and then iterate until the convergence of the density-dependent gaps in Eq. (8) is achieved. We have tested our SHF code and found that it agrees with similiar calculations [11,13].

The parameters ρ_0 and $V^{n,p}$ used in the present calculation are $\rho_0=0.16$ fm^{-3}, and $V_0^{n,p}=-650$, -500 MeV fm^{-3} for He, Li, and Be isotopes. The reference density $\rho_0=0.16$ fm^{-3} is close to the nuclear matter density. The strength V_0^τ for ρ_0 is determined so that the minimum of quasiparticle energies agrees well with experimental pairing gaps [11,14].

The center-of-mass correction is also important in light nuclei. We eliminate the spurious center-of-mass excitation by the method used in [9,10].

III. NUMERICAL RESULTS

We use the SHFDD model to calculate the ground-state properties of light nuclei He, Li, and Be. The numerical results on binding energies, pairing energies, and root-mean-square (rms) radii of matter, neutron, and proton distributions R_m, R_n, R_p, have been listed in Tables I–III for He, Li, and Be isotopes, respectively. The rms matter radius has been calculated by defining the total radius as the average of proton and neutron radii in every orbit weighted with occupation probabilities. Because the difference of single-particle energies between $1P_{3/2}$ and $1P_{1/2}$ is as high as 5–10 MeV for the above isotopes, the $1p_{3/2}$ level can be treated as a subshell and the influence of pairing forces is very small [15]. It is well known that the angular momentum and parity of nuclei with an odd nucleon outside a closed shell only

TABLE II. Binding energy, pairing energy, and various radii of Li isotopes. Experimental radii are taken from Ref. [1]. B and PE denote the binding energy and the pairing energy, respectively.

	Expt			SHFDD				
	B (MeV)	R_n (fm)	R_m (fm)	B (MeV)	PE (MeV)	R_n (fm)	R_m (fm)	R_p (fm)
^{6}Li	31.99	2.69±0.41	2.46±0.21	30.49	0.00	2.41	2.42	2.43
^{7}Li	39.27	2.52±0.06	2.39±0.02	37.21	2.49	2.60	2.48	2.30
^{8}Li	41.28	2.80±0.04	2.58±0.03	40.27	0.00	2.69	2.53	2.24
^{9}Li	45.34	2.70±0.04	2.54±0.03	45.84	0.01	2.76	2.59	2.20
^{10}Li	44.92			45.81	0.00	2.78	2.62	2.22
^{11}Li	45.65	2.96±0.10	2.78±0.07	47.95	0.00	3.06	2.87	2.28

depend on the occupation of the last neutron (or proton) while one valence nucleon (or one hole) is just outside a closed shell. So we do not take into account the effect of pairing forces for nuclei with a proton or a neutron outside a closed shell in our calculations. For example, the proton pairing force of ^{7}Li is chosen to be zero because there is one proton in $1p_{3/2}$, but its neutron pairing force has been taken into account. In calculations, a cutoff radius for radial integrations is chosen as 15 fm and this is a reasonably large value for the precision of calculations on exotic neutron-rich nuclei since outside neutrons in them are weakly bound.

Now let us give a detailed discussion on every isotope. The numerical results for He isotopes have been listed in Table I. It is seen from Table I that the binding energies from the SHFDD model agree well with experimental data [16]. The one-neutron separation energy of He isotopes is plotted in Fig. 1 where it has been defined as a difference of binding energies $S_n(Z,N)=B(Z,N)-B(Z,N-1)$. The experimental odd-even staggering is very well described by calculations. It should be noted that the neutron separation energy of ^{5}He, ^{7}He, and ^{9}He is negative. It means that these nuclei are unstable for one-neutron emission. For ^{10}He, all occupied single-particle states are bound in our calculation and the numerical result shows that ^{10}He is unstable for two-neutron emission because its binding energy is less than that of ^{8}He. These results agree with the experimental fact that ^{10}He has not been observed as a bound nucleus. The single-particle energies of neutrons in levels $1s_{1/2}$ and $1p_{3/2}$ for ^{6}He are, respectively, -16.45 MeV and -1.07 MeV. Those for ^{8}He are, respectively, -18.00 MeV and -2.01 MeV. These suggest that ^{6}He can be approximately considered as a ^{4}He core plus two neutrons and ^{8}He can be considered as a ^{4}He core plus four neutrons because outside neutrons are weakly bound. Therefore people can use a few-body model to investigate their ground state properties. It is seen from Fig. 2 that the density distribution of protons in ^{4}He, ^{6}He, and ^{8}He are approximately the same, but the density distribution of neutrons in ^{6}He and ^{8}He extends farther than that of ^{4}He. It indicates that the neutron and matter radii of ^{6}He and ^{8}He are abnormally larger than those of ^{4}He. For ^{6}He and ^{8}He, the mean-square radii of neutrons in the

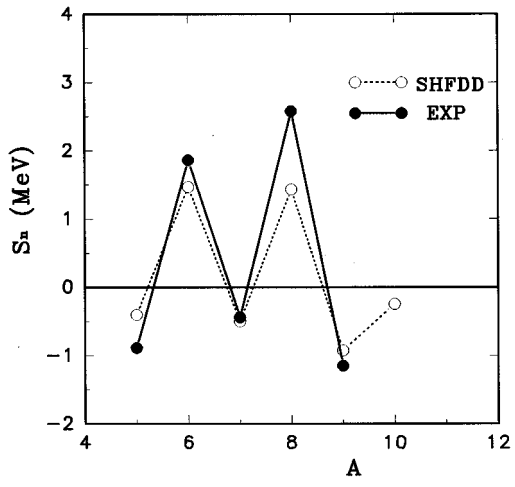

FIG. 1. Neutron separation energy of He isotopes. The hollow circles are calculated values obtained with SHFDD. Experimental values are denoted by a full circle.

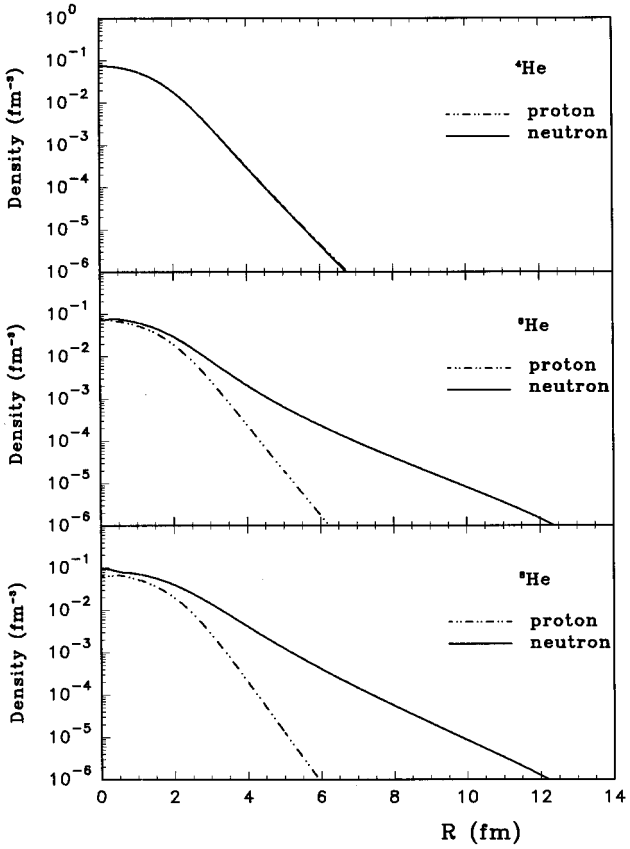

FIG. 2. Density distribution of protons and neutrons for ^{4}He, ^{6}He, and ^{8}He.

TABLE III. Same as Table II but for Be isotopes.

	Expt			SHFDD				
	B (MeV)	R_n (fm)	R_m (fm)	B (MeV)	PE (MeV)	R_n (fm)	R_m (fm)	R_p (fm)
^{7}Be	37.60			35.17	1.70	2.30	2.50	2.64
^{8}Be	56.50			46.14	4.05	2.43	2.43	2.44
^{9}Be	58.16	2.67±0.13	2.53±0.07	53.76	1.63	2.52	2.44	2.35
^{10}Be	64.97	2.59±0.05	2.48±0.03	63.49	1.55	2.58	2.48	2.31
^{11}Be	65.48	3.38±0.06	3.04±0.04	66.49	1.49	2.74	2.60	2.34
^{12}Be	68.65	2.75±0.11	2.62±0.07	69.79	1.43	2.83	2.68	2.37
^{14}Be	69.99	3.68±0.26	3.36±0.19	70.64	1.38	3.55	3.26	2.39

$1p_{3/2}$ level are, respectively, $\overline{R^2}(1p_{3/2})=15.06$ fm^2 and $\overline{R^2}(1p3/2)=13.69$ fm^2. They are abnormally large as compared with the square of neutron rms radii in ^{6}He and ^{8}He. It is concluded that there are two-neutron halos in ^{6}He and four-neutron halos in ^{8}He. As compared with the SHF model with standard force parameters, the SHFDD model with SKI4 has an isospin-dependent spin-orbit interaction. We can reproduce experimental data well with the SHFDD theory because the influence from the isospin degree of freedom is included and the neutron-neutron correlation is carefully treated.

The numerical results of Li and Be isotopes are listed in Tables II and III, respectively. That the theoretical binding energy of ^{10}Li is lower than that of ^{9}Li means that ^{10}Li is unstable for one-neutron emission. This agrees with experimental facts. ^{11}Li can be considered as a ^{9}Li core plus two halo neutrons [17]. The density distributions of Li isotopes have been also plotted in Fig. 3. It is seen from Fig. 3 that the neutron density distributions in ^{7}Li and ^{9}Li are approximately the same. Neutrons in ^{11}Li have an extended distribution up to 11 fm. The mean-square radius of neutrons in the $1p_{1/2}$ level is $\overline{R^2}(1p_{1/2})=14.0$ fm^2 in the present calculation.

Because the last neutron orbit in ^{13}Be is unbound in our calculations, we have not given the result of ^{13}Be in Table III. It is well known that ^{13}Be is unbound. The theoretical binding energy of ^{8}Be is 10 MeV lower than the empirical value since there exist alpha correlations or large deformations in ^{8}Be. They are not included in the present calculation. Because the binding energy of ^{8}Be is less than twice of the binding energy of ^{4}He, ^{8}Be is unstable to alpha emission and this agrees with experimental facts. It is seen from Table III that experimental data for ^{14}Be are reproduced so well in the SHFDD model due to the use of a density-dependent pairing force. This is the first time that the neutron halo of ^{14}Be is reproduced within the SHF theory without any parameter fitting or introducing an artificial infinite well at a large radius. In order to illustrate this problem further, in Table IV, we have listed the results calculated by the density-dependent pairing correlation, by the constant-gap approach, by the constant-force approach and by a zero-pairing force approach of neutrons for comparison. Case (a) is the constant-gap approach with $\Delta^{\tau}=11.2/\sqrt{A}$ MeV where the superscript $\tau=n$ (p) denotes the neutrons (protons) [12]. Case (b) is the constant-force approach with $G_P=16.5/(11+Z)$ MeV for protons and $G_n=13.5/(11+N)$ MeV for neutrons [14]. Case (c) is the result in which the neutron pairing force has been switched off and the proton pairing force is treated as in case (a). In all cases, the calculated results are obtained with the SKI4 parameter set. We have seen from Table IV that the level of outer neutrons is unbound in cases (a), (b), and (c) and this shows that the SHF model with ordinary pairing forces fails for ^{14}Be. The results in cases (a), (b), and (c) are only used as an explanation in our calculations for ^{14}Be because outer neutron levels are unbound. The SHFDD results of ^{14}Be agree well with experimental data not only for the binding energy but also for the neutron and matter radii. As the single-particle energy of $2s_{1/2}$ is negative in the SHFDD model, the level $2s_{1/2}$ is bound for ^{14}Be. Furthermore, the occupying weights in levels $1d_{5/2}$ and $1d_{3/2}$ are close to zero. It means the two outer neutrons in ^{14}Be will occupy the level $2s_{1/2}$ and this agrees

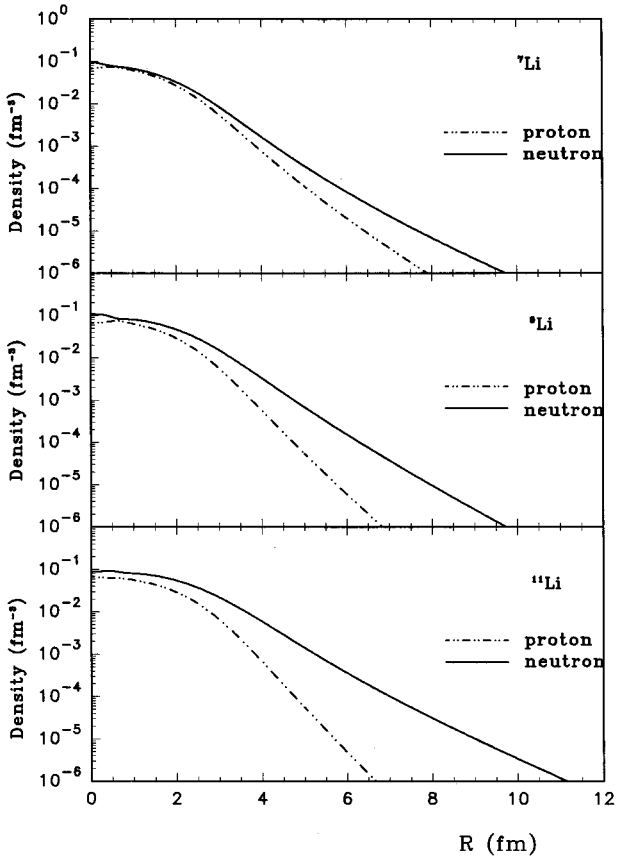

FIG. 3. Density distribution of protons and neutrons for ^{7}Li, ^{9}Li, and ^{11}Li.

TABLE IV. Numerical results for ^{14}Be. B(expt) = 69.99 MeV [16], R_n(expt) = 3.68 ± 0.38 fm, R_m(expt) = 3.36 ± 0.19 fm [1]. The quantities in brackets are occupying weights of single-particle levels.

	SHFDD	(a)	(b)	(c)
B (MeV)	70.64	72.27	68.03	68.99
R_m (fm)	3.26	3.94	3.75	3.62
R_n (fm)	3.55	4.42	4.18	4.00
R_p (fm)	2.39	2.40	2.39	2.40
$\epsilon(1s_{1/2})(p)$	-38.06(1.00)	-36.02(0.99)	-36.52(1.00)	-36.45(0.99)
$\epsilon(1p_{3/2})(p)$	-20.43(0.50)	-19.48(0.48)	-19.99(0.50)	-19.90(0.48)
$\epsilon(1p_{1/2})(p)$	-13.22(~0.0)	-12.67(0.04)	-13.01(~0.0)	-12.87(0.04)
$\epsilon(1s_{1/2})(n)$	-30.54(1.00)	-28.49(1.00)	-28.70(1.00)	-28.40(1.00)
$\epsilon(1p_{3/2})(n)$	-10.48(1.00)	-10.01(0.98)	-10.16(1.00)	-10.19(1.00)
$\epsilon(1p_{1/2})(n)$	-5.74(1.00)	-5.40(0.92)	-5.51(0.99)	-5.55(1.00)
$\epsilon(2s_{1/2})(n)$	-0.24(1.00)	0.12(0.38)	0.10(0.57)	0.10(1.00)
$\epsilon(2d_{5/2})(n)$	2.01(~0.0)	2.15(0.16)	2.12(0.10)	
$\epsilon(2d_{3/2})(n)$	2.68(~0.0)	2.69(0.13)	2.68(0.07)	

with the recent results obtained with the density-dependent relativistic mean-field theory [18] and with a three-body model [20]. It is worthy to analyse why the density-dependent pairing force can reproduce experimental data of ^{14}Be very well. The reason is that the neutron-neutron correlation is carefully considered in the present calculation. The neutron-neutron correlation becomes more and more important in a low density range. The neutron-neutron correlation has an influence on the mean field of halo nucleus ^{14}Be so that the level $2s_{1/2}$ is bound. This also avoids the unphysical occupation of neutron pairs in positive-energy orbits and keeps the neutrons from escaping. This picture consists with that from the density-dependent relativistic mean field theory [18] and it shows that the mean-field is varying for halo nuclei [4,5,18]. In order to see the appearance of the neutron halo for ^{14}Be in the SHFDD theory more clearly, we also give the density distributions of protons and neutrons in ^{10}Be, ^{12}Be, and ^{14}Be in Fig. 4. It is clearly seen that there are neutron halos in ^{14}Be.

In order to see the effect of the modified spin-orbit interaction in SKI4 clearly, let us compare the present results with those obtained with the other Skyrme-type parameter sets. We choose two Skyrme-type sets SKI2 and SKI3 for comparison which are also given by Reinhard *et al.* [12]. Among SKI2, SKI3, and SKI4, an important difference is the spin-orbit interaction. The parameter set SKI2, which is similar to the standard Skyrme functional, has a spin-orbit potential proportional to $2\rho+\rho_q$, where $q=p$ (n) denotes protons (neutrons) [12]. For the parameter set SKI3, $b_4'=0$, the spin-orbit potential is proportional to $\rho=\rho_n+\rho_p$ [12] and this structure of spin-orbit potentials lies between SKI2 and SKI4. The theoretical binding energies of He, Li, and Be nuclei with three sets of parameters, SKI2, SKI3, and SKI4, are plotted in Fig. 5. In calculations, a density-dependent pairing correlation has been inputted. It is obvious that the results obtained with SKI2 are more off experimental data than those of SKI3 and SKI4, especially for nuclei far from the line of stability. The result from SKI4 is the best one as compared with experimental data. The theoretical results of ^{14}Be with SKI3 are not given in the figure as its last orbit is unbound. Although SKI2 can give the result of ^{14}Be in Fig. 5, the binding energy of ^{12}Be is larger than that of ^{14}Be. It means that ^{14}Be is unstable for two-neutron emission and this does not agree with experiment facts. From Table V, we can clearly see this again. It is concluded that SKI4 works best among those parameter sets. In the set SKI4, the neutron spin-orbit potential is proportional to ρ_p and the proton one is proportional to ρ_n. In this structure of spin-orbit potentials, a neutron-proton interaction has been effectively taken

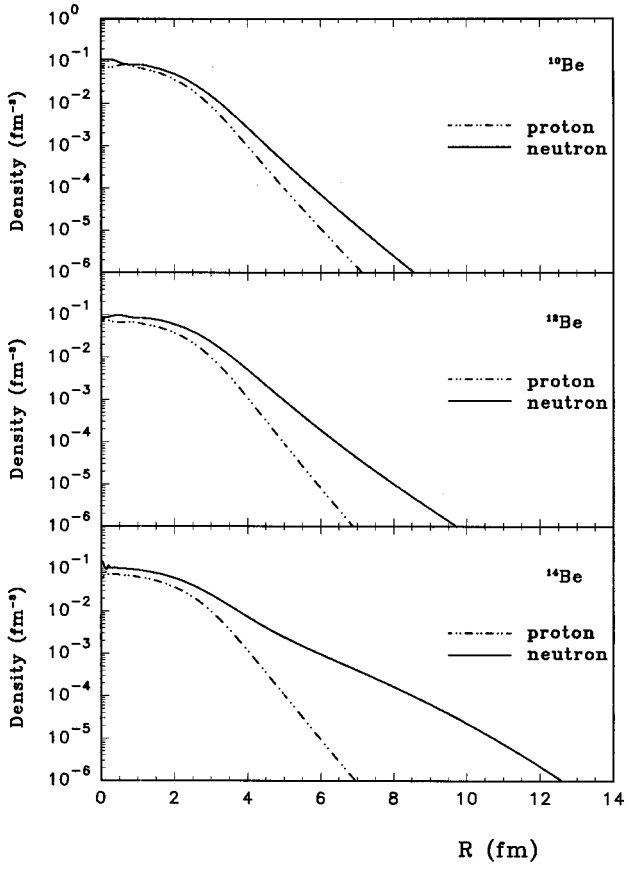

FIG. 4. Density distribution of protons and neutrons for ^{10}Be, ^{12}Be, and ^{14}Be.

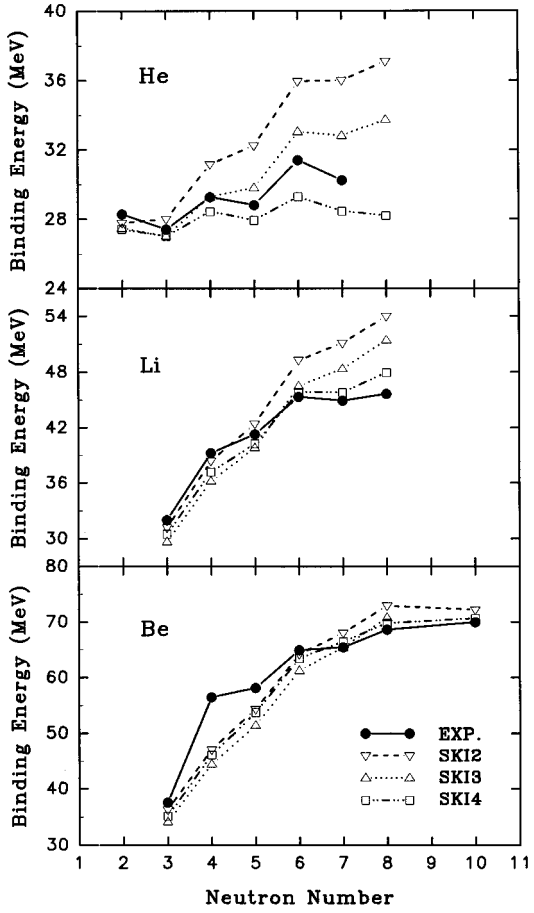

FIG. 5. Binding energy for He, Li, and Be isotopes with Skyrme-type parameter sets SKI2, SKI3, and SKI4.

into account for nuclei far from the line of stability and so it gives a correct picture for nuclei in this region.

Finally we have drawn theoretical and experimental neutron radii of Li and Be isotopes in Fig. 6. The numerical results from the SHFDD theory with SKI4 agree with experimental data except for halo nucleus ^{11}Be. For ^{11}Be, the spin and parity of the ground state are $1/2^-$ in our calculation. The state $1/2^+$ is an excited state of ^{11}Be and its single-

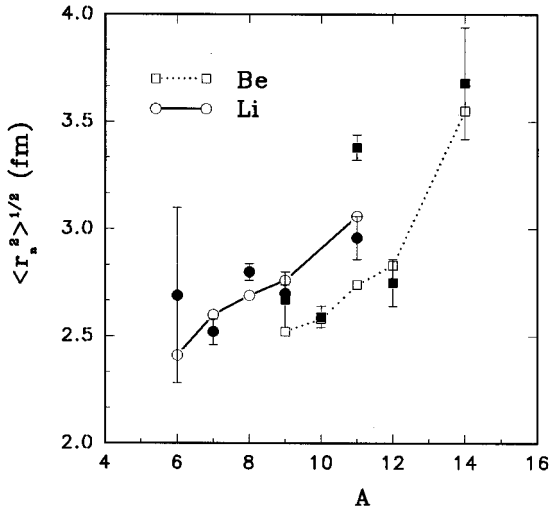

FIG. 6. Comparison between experimental and theoretical neutron radii which is plotted with the mass number A. The full circle and full diamond symbols correspond to experimental values of Li and Be, respectively. The hollow circle and hollow diamond symbols correspond to theoretical values of Li and Be, respectively. The experimental data are taken from Liatard *et al.* [1].

particle energy is positive. The experimental ground state of ^{11}Be is $1/2^+$. This disagreement between the theoretical ground state and experimental one may be the cause why the model cannot reproduce a one-neutron halo in ^{11}Be. Although we cannot give the experimental spin and parity for the ground state of ^{11}Be, this does not have an influence on the explanation of neutron halos in other nuclei [4,5,19,20]. Bertsch *et al.* [4,5] and Zhu *et al.* [19] have shown that one can reproduce the neutron halo of ^{11}Li and ^{14}Be well even if the experimental ground state of ^{11}Be cannot be reproduced. Thompson and Zhukov have also confirmed this very recently [20].

In a word, the SHFDD results of He, Li, and Be isotopes agree well with experimental data on binding energies and radii. It also succeeds in explaining neutron halos in nuclei ^{6}He, ^{8}He, ^{11}Li, and ^{14}Be except that in ^{11}Be. The SHFDD model can give reliable results for exotic light neutron-rich

TABLE V. Numerical results for ^{12}Be and ^{14}Be calculated with Skyrme-type parameter sets SKI2, SKI3, and SKI4. The experimental values for Be nuclei are listed in Table III. The quantities in brackets are occupying weights of single-particle levels.

	SKI2		SKI3		SKI4	
	^{12}Be	^{14}Be	^{12}Be	^{14}Be	^{12}Be	^{14}Be
B (MeV)	72.94	72.23	70.80	68.96	69.79	70.64
R_m (fm)	2.67	3.31	2.65	3.84	2.68	3.26
R_n (fm)	2.81	3.62	2.77	4.28	2.83	3.55
R_p (fm)	2.37	2.39	2.38	2.40	2.37	2.39
$\epsilon(1s_{1/2})(n)$	-28.35	-28.56(1.00)	-32.51	-32.61(1.00)	-30.45	-30.54(1.00)
$\epsilon(1p_{3/2})(n)$	-11.25	-11.98(1.00)	-12.00	-12.26(1.00)	-10.26	-10.48(1.00)
$\epsilon(1p_{1/2})(n)$	-5.82	-6.64(0.99)	-6.35	-6.63(1.00)	-5.00	-5.74(1.00)
$\epsilon(2s_{1/2})(n)$		-0.44(0.62)		0.08(1.00)		-0.24(1.00)
$\epsilon(2d_{5/2})(n)$		0.72(0.13)		1.62($\sim$0.0)		2.01($\sim$0.0)
$\epsilon(2d_{3/2})(n)$		2.55(0.01)		2.09($\sim$0.0)		2.68($\sim$0.0)

nuclei because the nucleon-nucleon correlations have been treated carefully and the isospin degree of freedom has also been included in the force parameters. To develop the present SHFDD model further and to incorporate the correlations beyond the mean field such as proton-neutron correlations and alpha correlations will be a future task.

IV. CONCLUSIONS

In this paper, we have successfully reproduced experimental binding energies and radii, and neutron halos in nuclei ^{6}He, ^{8}He, ^{11}Li, ^{14}Be using the SHFDD model with SKI4. The odd-even staggering of neutron separation energies in He isotopes has also been successfully obtained. The nucleus ^{10}He is unstable for two-neutron emission and ^{10}Li is unstable for one-neutron emission. This also agrees with experimental facts. The above success is due to following two facts: one is that the isospin degree of freedom has been correctly included in the mean field; the other is that the nucleon-nucleon correlation is carefully treated by introducing a density-dependent pairing force as compared with the standard SHF model with the constant-gap approach or with the constant-force approach. In the future, it will be interesting to develop the present SHFDD model for deformed nuclei.

[1] E. Liatard *et al.*, Europhys. Lett **13**, 401 (1990).
[2] W. Mittig *et al.*, Phys. Rev. Lett. **59**, 592 (1987).
[3] M. G. Saint-Laurent *et al.*, Z. Phys. A **332**, 457 (1989).
[4] G. F. Bertsch and H. Esbensen, Ann. Phys. **209**, 327 (1991).
[5] G. F. Bertsch *et al.*, Phys. Rev. C **39**, 1154 (1989).
[6] D. Vautherm and D. M. Brink, Phys. Rev. C **5**, 626 (1972).
[7] J. Dobaczewski, I. Hamamoto, W. Nazarewicz, and J.A. Sheikh, Phys. Rev. Lett **72**, 981 (1994).
[8] J. Friedrich and P. G. Reinhard, Phys. Rev. C **33**, 335 (1986).
[9] H. Sagawa and H. Toki, J. Phys. G **13**, 453 (1987).
[10] P. G. Reinhard, F. Hummer, and K. Goeke, Z. Phys. A **317**, 339 (1984).
[11] N. Tajima, P. Bonche, H. Flocard, P. H. Heenen, and M. S. Weiss, Nucl. Phys. **A551**, 434 (1993).
[12] P. G. Reinhard and H. Flocard, Nucl. Phys. **A584**, 467 (1995).
[13] S. J. Krieger, P. Bonche, H. Flocard, P. Quentin, and M. S. Weiss, Nucl. Phys. **A517**, 275 (1990).
[14] P. Bonche, H. Flocard, P. H. Heenen, S. J. Krieger, and M. S. Weiss, Nucl. Phys. **A443**, 39 (1985).
[15] Yao-song Shen and Zhongzhou Ren, Commun. Theor. Phys. (to be published).
[16] G. Audi and A. H. Wapstra, Nucl. Phys. **A565**, 1 (1993).
[17] F. Pougheon, Z. Phys. A **349**, 273 (1994).
[18] Zhongzhou Ren, Gongou Xu, Baoqiu Chen, Zhongyu Ma, and W. Mittig, Phys. Lett. B **351**, 11 (1995).
[19] Z. Y. Zhu, W. Q. Shen, Y. H. Cai, and Y. G. Ma, Phys. Lett. B **328**, 1 (1994)
[20] I. J. Thompson and M.V. Zhukov, Phys. Rev. C **53**, 708 (1996), see conclusion on p. 713.